

## Synthesis of cubic diamond in the graphite-magnesium carbonate and graphite-K<sub>2</sub>Mg(CO<sub>3</sub>)<sub>2</sub> systems at high pressure of 9–10 GPa region

T. Taniguchi

National Institute for Research in Inorganic Materials, 1-1 Namiki Tsukuba Ibaraki 305, Japan

D. Dobson, A. P. Jones, R. Rabe, and H. J. Milledge

Department of Geophysical and Geological Science, University College London, Gower Street, London WC1E 6BT, United Kingdom

(Received 9 August 1995; accepted 6 April 1996)

Cubic diamond was synthesized with two systems, (1) graphite with pure magnesium carbonate (magnesite) and (2) graphite with mixed potassium and magnesium carbonate at pressures and temperatures above 9.5 GPa, 1600 °C and 9 GPa, 1650 °C, respectively. At these conditions (1) the pure magnesite is solid, whereas (2) the mixed carbonate exists as a melt. In this pressure range, graphite seems to be partially transformed into hexagonal diamond. Measured carbon isotope  $\delta^{13}\text{C}$  values for all the materials suggest that the origin of the carbon source to form cubic diamond was the initial graphite powder, and not the carbonates.

### I. INTRODUCTION

Recently, it has been reported that the conversion reaction from graphite to diamond takes place at high pressure (HP) (8 GPa) and high temperature (HT) (2100 °C) in the presence of some inorganic compounds as solvent catalyst.<sup>1–3</sup> Following the first discovery, several experimental investigations for the growth and nucleation of synthetic diamond with the inorganic compounds have been reported.<sup>4–6</sup>

Among the several inorganic compounds identified in these pilot studies, the graphite-carbonate system is particularly interesting, because carbonate minerals are common in the earth. The reported studies for the carbonate-graphite system have been carried out in the pressure range up to 8 GPa at HT near 2150 °C.<sup>1,3</sup> As mentioned in these papers, the synthesis temperature for diamond in this system is much higher than that for the formation of natural diamond. However, it was found in the other inorganic compound catalyst system that the lower boundary of the synthesis temperature for diamond becomes lower as the pressure is increased.<sup>3</sup> In order to clarify the reaction boundary for diamond formation in the presence of carbonate, it is important to carry out synthesis experiments under a wider range of pressures.

On the other hand, the lower limit of temperature required to form diamond has been considered to be related to the melting temperature of the catalytic solvent materials.<sup>7</sup> It is known that the melting temperature of binary carbonate systems becomes lower by involving an alkali component due to their eutectic or peritectic relationship.<sup>8</sup> Therefore, the study of the formation of diamond in the mixed carbonate system with a eutectic

relationship is interesting for determining the lower boundary of reaction temperature.

With the above perspective, we carried out an investigation to realize the synthesis of diamond with two systems: (1) graphite-magnesium carbonate and (2) graphite-potassium and magnesium carbonate at pressures and temperatures in the range of 9–10 GPa and 1500–1800 °C. In order to clarify the effect of addition of the carbonate on the formation of diamond in these systems, HP and HT treatment for pure graphite powder was also performed. Furthermore, to understand the transformation process of diamond in these systems, carbon isotope analyses have been carried out for synthesized diamond as well as all the starting materials in the present study.

### II. EXPERIMENTAL

#### A. Starting materials

Starting materials used were high purity graphite (UCP1-100: supplied by Ultra Carbon Corp.: impurity concentration less than 5 ppm, graphitized index (G.I.)<sup>9</sup> value was 7.4), natural magnesium carbonate [MgCO<sub>3</sub>: origin of New South Wales (hereafter denoted as NSW), Australia], and potassium carbonate (K<sub>2</sub>CO<sub>3</sub>: BDH Limited AnalaR, 99.9%). In the system graphite-MgCO<sub>3</sub>, powdered MgCO<sub>3</sub> was mixed in 1 : 1 weight ratio with graphite. X-ray diffraction profiles of the graphite and system graphite-MgCO<sub>3</sub> as starting materials are shown in Figs. 1(a) and 1(b), respectively. To check the composition and identify impurities in the natural MgCO<sub>3</sub> as a starting material, another natural MgCO<sub>3</sub> from

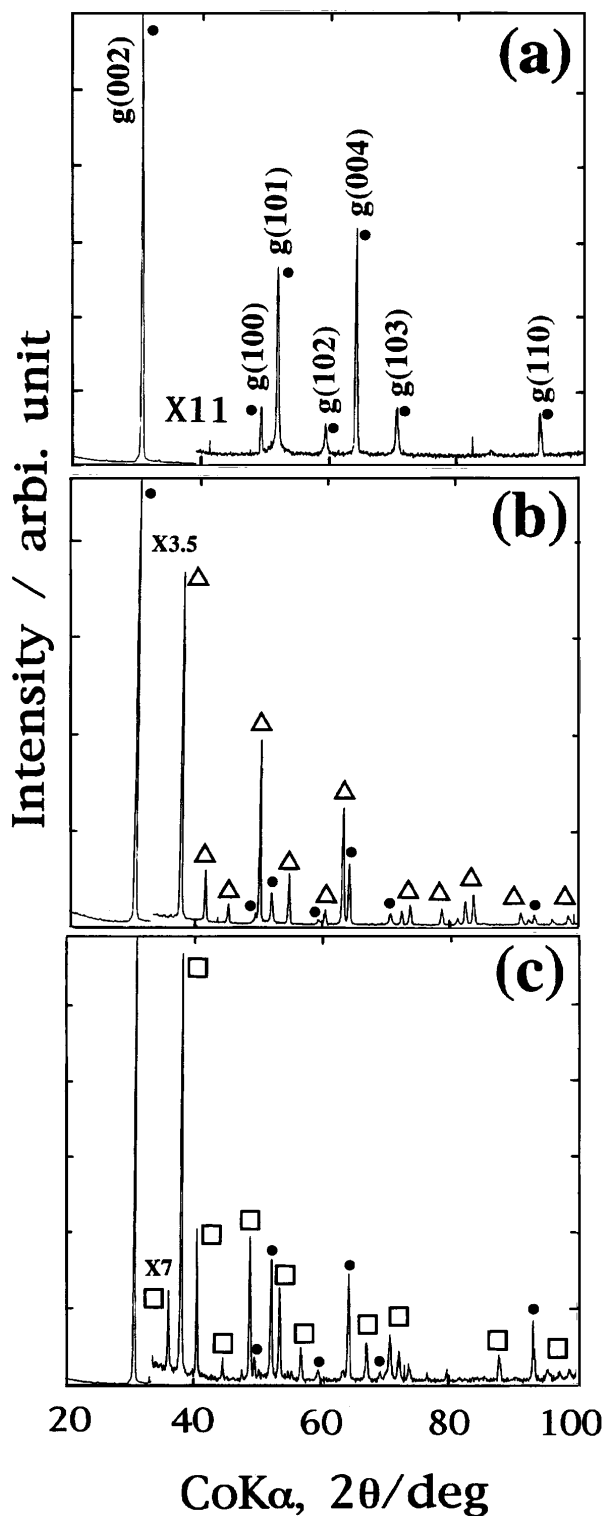


FIG. 1. X-ray diffraction profiles of the starting materials. (a) graphite, (b) system graphite-MgCO<sub>3</sub>, and (c) system graphite-K<sub>2</sub>Mg(CO<sub>3</sub>)<sub>2</sub>. (●) graphite, (△) MgCO<sub>3</sub>, and (□) K<sub>2</sub>Mg(CO<sub>3</sub>)<sub>2</sub>.

San Bernardino County, California, USA, and laboratory made MgCO<sub>3</sub><sup>10</sup> were also used. Thus, three types of magnesite were used in all. According to Electron Probe

Micro Analysis (EPMA),<sup>11</sup> detectable impurity in the MgCO<sub>3</sub> from NSW and that from California were Ca (0.5 atm %) and Na (0.1 atm %), and Ca (1.5 atm %), Si (0.2 atm %), and Na (0.1 atm %), respectively. In the analysis, beam current was 15 keV and energy dispersive spectra were collected for 100 s. These operating conditions produce a precision of 0.1 atm % for carbonate samples. Inductively coupled plasma emission spectroscopy (ICP) analysis was also performed for all the starting materials listed above to check the impurity of Fe, Ni, and Co, which is a well-known catalyst for the formation of c-diamond. Consequently, the amount of these impurities was defined to be less than 0.005 wt. %.

In the system K<sub>2</sub>CO<sub>3</sub>-MgCO<sub>3</sub>-C, it is not easy to eliminate the effect of a hydrous component in K<sub>2</sub>CO<sub>3</sub>, because this alkali-carbonate is strongly hydroscopic. In order to minimize this effect, an intermediate compound, potassium-magnesium carbonate [K<sub>2</sub>Mg(CO<sub>3</sub>)<sub>2</sub>], was synthesized by using a piston cylinder apparatus.<sup>12</sup> A stoichiometric mixture of dried K<sub>2</sub>CO<sub>3</sub> and MgCO<sub>3</sub> powder was packed in a graphite capsule and treated at 750 °C for 30 min and 300 °C for 5 h under pressure of 0.25 GPa. No water was detected in either the MgCO<sub>3</sub> or the synthetic K<sub>2</sub>Mg(CO<sub>3</sub>)<sub>2</sub> by infrared (IR) spectroscopy. In the system graphite-K<sub>2</sub>Mg(CO<sub>3</sub>)<sub>2</sub>, powdered K<sub>2</sub>Mg(CO<sub>3</sub>)<sub>2</sub> was mixed in 1:1 weight ratio with graphite as a starting material. An x-ray diffraction profile of the system graphite-K<sub>2</sub>Mg(CO<sub>3</sub>)<sub>2</sub> is shown in Fig. 1(c).

## B. High-pressure experiments

High-pressure experiments were performed by a modified double-stage HP apparatus for piston cylinder laboratories.<sup>13</sup> The assembled double-stage module is basically similar to the well-known 6-8 type HP device.<sup>14</sup> The cubic inner anvils were 25.5 mm edge length with 8 mm truncated edge length. Octahedra of cast magnesium oxide with an edge length of 13 mm were used as a pressure transmitting medium combined with pyrophyllite fin gaskets. Pressure calibration has been made at room temperature using the phase transitions: Bi-II (2.55 GPa), BiIII-V (7.7 GPa), and Sn (9.4 GPa). Pressure calibrations at 1100 °C and 5 GPa and at 1100 °C and 1500 °C at 9 GPa have also been made by using the phase transformations  $\alpha$ - $\gamma$ Fe<sub>2</sub>SiO<sub>4</sub><sup>15</sup> and coesite-stishovite,<sup>16</sup> respectively.

The sample assembly used is shown in Fig. 2. The cylindrical graphite furnace with 3.4 mm inner diameter and 7 mm length is surrounded by a zirconium oxide thermal insulator. Pure graphite powder (UCP1-100), the system graphite-MgCO<sub>3</sub>, and graphite-K<sub>2</sub>Mg(CO<sub>3</sub>)<sub>2</sub> as starting materials were dried at 120 °C and packed in a graphite capsule whose size was 1.5 mm inner diameter and 1.6 mm in length. In each HP/HT experiment,

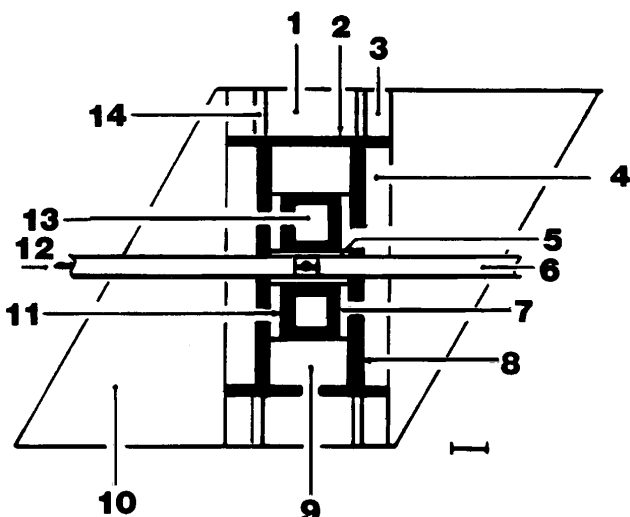


FIG. 2. Cross section of octahedral sample cell assembly. 1: zirconium oxide ( $ZrO_2$ ) end plug, 2: graphite plate, 3: pyrophyllite ring, 4:  $ZrO_2$  thermal insulating sleeve, 5: hexagonal boron nitride plate, 6: alumina insulating sleeve, 7: alumina sleeve, 8: graphite heater, 9:  $ZrO_2$  thermal insulating plug, 10: cast magnesium oxide octahedral, 11: graphite capsule, 12: Pt/Rh6–30% thermocouple, 13: sample, and 14: copper current ring. Bar indicates 1 mm.

two sample capsules were simultaneously treated, as shown in Fig. 2. The graphite furnace and capsule were machined from graphite rod (G-530 type supplied by Tokai Carbon Co.) whose bulk density and ash content were  $1.82\text{ g/cm}^3$  and 0.1%, respectively. The G.I. value of the graphite rod was infinite due to a lack of the (102) peak in its x-ray diffraction pattern. Experimental durations at HP/HT were fixed to 20 min after which the sample was quenched by shutting off the electrical power. Temperature was measured using Pt-Rh/6–30 wt. % type thermocouples in each experiment. Correction for any pressure effect on the emf of the thermocouples was not made. The temperature gradient of the sample space was characterized by running a geothermometer of the mixture of enstatite-diopside 1 : 1 mol % at 5.5 GPa and  $1500\text{ }^\circ\text{C}$ .<sup>17</sup> The Ca contents of diopsidic clinopyroxene coexisting with orthopyroxene are known to be a good indicator of equilibrium temperatures. The temperature distribution in the furnace assembly can be, therefore, monitored by analyzing synthesized pyroxene compositions as a function of location which can be evaluated by EPMA analysis. According to the analysis, the temperature gradient in the sample space is calculated to be less than  $150\text{ }^\circ\text{C/mm}$  along the length of the sample space. Since the thermocouple was located in the center of the hottest region in the furnace, the temperature measured with the thermocouple represents the upper bound of the temperature of the sample space.

Characterization of the recovered sample was performed with powder x-ray diffraction experiment, cathodoluminescence (CL) spectroscopy, EPMA, and

scanning electron microscopy (SEM) observation. In some experiments, additional characterization was made with a crushed grain mount under oil using a petrological microscope. Acid treatment was performed to dissolve carbonate and graphite by solution in hot aqua regia and a hot mixture of  $HNO_3$  and  $H_2SO_4$ , respectively.

Carbon isotope analysis for  $\delta^{13}\text{C}$  value was also carried out to investigate the origin of the carbon source for the diamond produced in the present systems. The measurement of  $\delta^{13}\text{C}$  value on all the starting materials and a range of purified run products was performed by mass spectroscopy at the Open University, courtesy of Professor C. T. Pillinger.<sup>18</sup>

### III. RESULTS AND DISCUSSION

#### A. High pressure/high-temperature treatment of pure graphite

Figure 3 shows the x-ray diffraction profiles of powdered pure graphite of quenched products after HP/HT treatment. It is worth noticing that the initial graphite was not essentially changed at room temperature and 11 GPa, but partially changed its structure at  $1100\text{ }^\circ\text{C}$  and the 9.5 GPa region. The compressed graphite [as indicated by an arrow in Fig. 3(c)] and the broadened peaks, which correspond to peaks assigned as h(100) and h(002) for hexagonal diamond (hereafter denoted as h-diamond) were seen in the recovered products. It is difficult to recognize the formation of cubic diamond (hereafter denoted as c-diamond) only from the x-ray diffraction pattern, because the peaks denoted as c(111) and c(220) for c-diamond overlap with h(002) and h(110), respectively.

On the contrary, the graphite capsule containing the powdered graphite has not undergone transformation to a dense phase, as described in the Appendix.

#### B. High-pressure/high-temperature treatment of the system graphite- $MgCO_3$

Figure 4 shows x-ray diffraction profiles of the powdered quenched products of the system graphite- $MgCO_3$ . As compared to Fig. 1(b), Fig. 4 shows significant catalytic effect, forming c-diamond with  $MgCO_3$  at 9.5 GPa and above  $1600\text{ }^\circ\text{C}$ . The x-ray diffraction profile of the  $MgCO_3$  phase accompanying the c-diamond formation was not changed from the starting condition, as shown in Fig. 4.

After HP/HT treatment, the sample was a solid lump which was mechanically removed from graphite capsule for characterization. Figure 5 shows optical photographs with CL color image of (a) the c-diamond grain aggregate after acid treatment and (b) a sectioned view of the sample in the recovered condition. The specimen after acid treatment as shown in Fig. 5(a) consists of single phase of c-diamond as measured

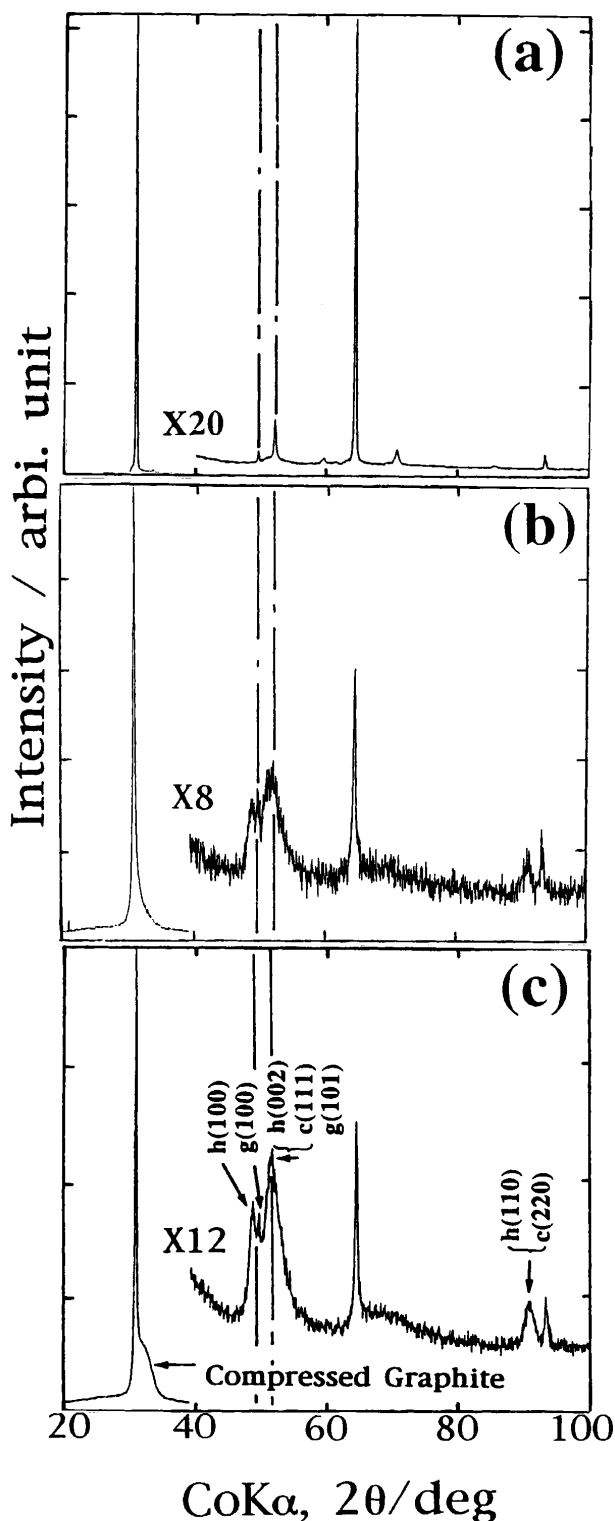


FIG. 3. X-ray diffraction profiles of the pure graphite. (a) HP treatment at 11 GPa and 25 °C for 20 min, (b) 9.5 GPa and 1100 °C for 20 min, and (c) 9.5 GPa and 1750 °C for 20 min.

by x-ray diffraction. Figure 5(b), yellow color part, located at the hot edge region in the capsule near the thermocouple, represents the existence of c-diamond

grain while red and black colors refer to MgCO<sub>3</sub> and graphite, respectively.

For the characterization using powder x-ray diffraction, the whole recovered sample was crushed into powder. The evaluation in this study, therefore, involves spatial heterogeneities of the c-diamond formation due to the temperature gradient, as shown in Fig. 5(b). The experimental results characterized by powder x-ray diffraction are summarized in Fig. 6. Each rectangle symbol in the P-T plane corresponds to the gradient of the formation of the c-diamond as typically exhibited in Fig. 5(b). The length of the sample capsule after HP/HT treatment was approximately 1.2 mm. Taking into account the temperature gradient in the capsule evaluated with the geothermometer as mentioned before, the maximum temperature gradient in the sample space should be less than 200 °C. Figure 6, therefore shows general trends of the formation of c-diamond in the system graphite-MgCO<sub>3</sub> at 9–10 GPa and 1300–1750 °C. No c-diamond formation has been observed in the quenched product from 9 GPa and under 1750 °C, while the c-diamond was synthesized above 9.5 GPa and 1600 °C.

In the system graphite-MgCO<sub>3</sub>, it has been reported that MgCO<sub>3</sub> has a catalytic effect for the formation of c-diamond and is an efficient sintering agent for diamond powder at 7.7 GPa and 2100 °C.<sup>3</sup> At this temperature, c-diamond in the system is a liquidus phase because MgCO<sub>3</sub> melts about 1900 °C at 7.7 GPa.<sup>19</sup> On the contrary, at 9.5 GPa, although the expected melting temperature of MgCO<sub>3</sub> is about 2000 °C,<sup>19</sup> the lower temperature limit for synthesizing c-diamond was about 1600 °C, as shown in Fig. 6. At this HP/HT condition, similar results have been obtained by using the different sources of MgCO<sub>3</sub> from California, and those that were laboratory made, as described in the Sec. II. A, though the yield of c-diamond was slightly changed.

SEM photographs of the samples of the system graphite-MgCO<sub>3</sub> are shown in Figs. 7(a–c). The photographs were taken near the central axis at the hot end of the sample. It can be seen that visible grains of MgCO<sub>3</sub>, which existed among the synthesized c-diamond grains, were dissolved leaving voids in the solid sample lump after acid treatment, as shown in Figs. 7 (a) and 7(b). The c-diamond formed from the system exhibited an average size of 1 μm or less with a not-well-formed crystal shape, as shown in Fig. 7(c).

### C. High-pressure/high-temperature treatment of the system graphite-K<sub>2</sub>Mg(CO<sub>3</sub>)<sub>2</sub>

Figure 8 shows x-ray diffraction profiles of the powdered quenched products of the system graphite-K<sub>2</sub>Mg(CO<sub>3</sub>)<sub>2</sub>. As compared to Fig. 1(c), Fig. 8 shows a significant catalytic effect, forming c-diamond with

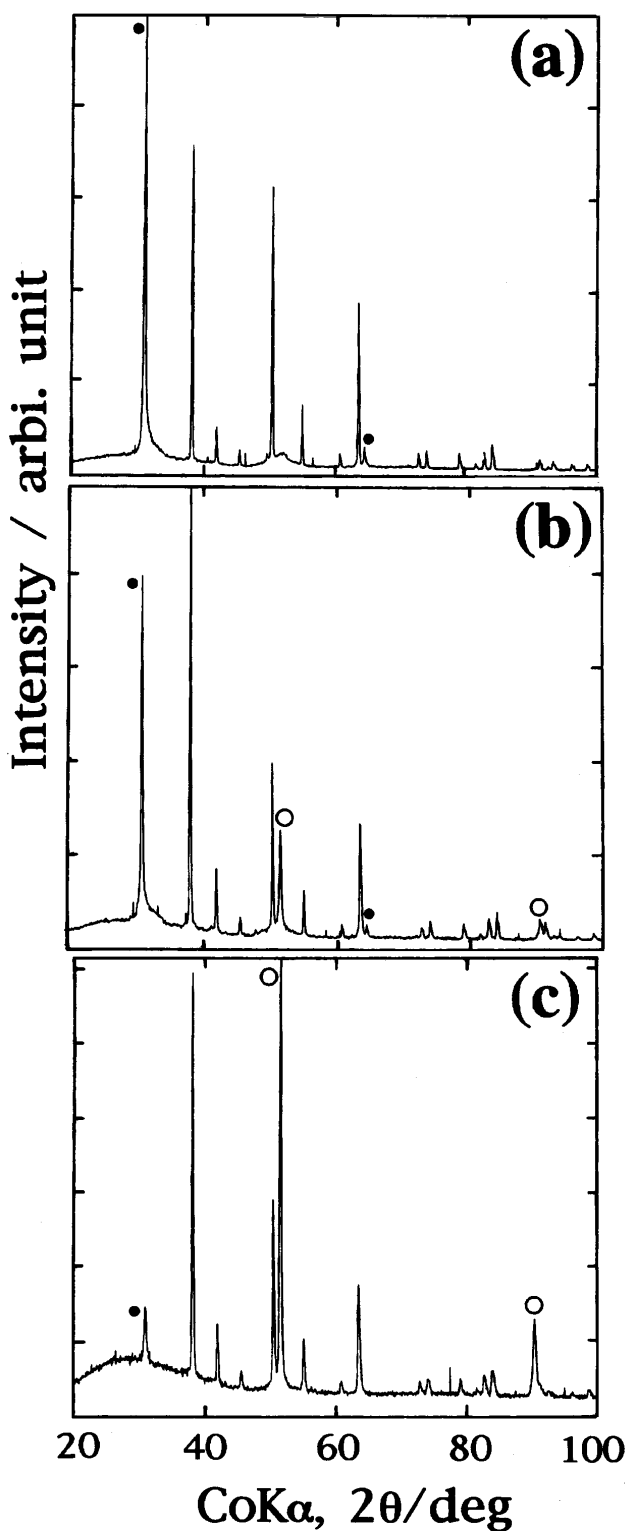


FIG. 4. X-ray diffraction profiles of the system graphite-MgCO<sub>3</sub>. (a) HP/HT treatment at 9.5 GPa and 1550 °C for 20 min, (b) 9.5 GPa and 1600 °C for 20 min, and (c) 9.5 GPa and 1650 °C for 20 min. (●) graphite and (○) c-diamond.

K<sub>2</sub>Mg(CO<sub>3</sub>)<sub>2</sub> at 9 GPa and above 1700 °C. The x-ray diffraction profile of the K<sub>2</sub>Mg(CO<sub>3</sub>)<sub>2</sub> phase accompany-

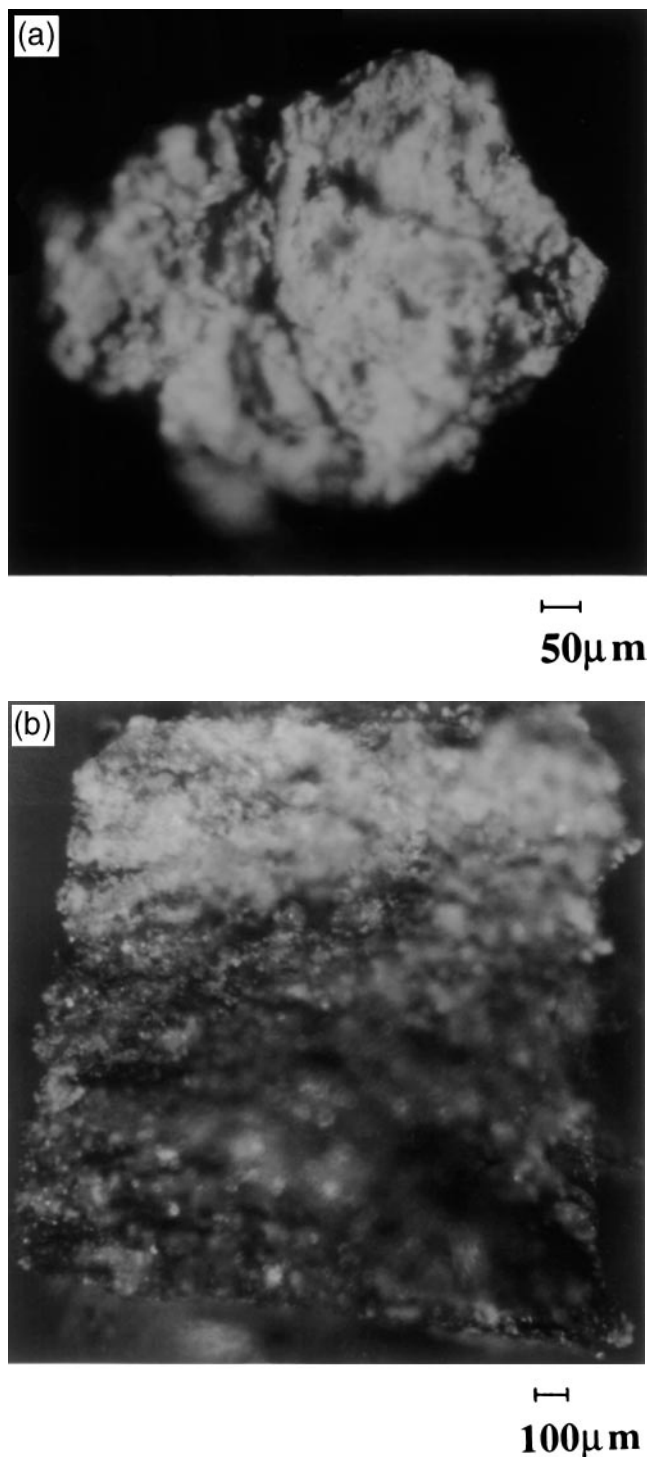


FIG. 5. Cathodoluminescence color image of recovered products of the system graphite-MgCO<sub>3</sub>. (a) c-diamond powder aggregate after acid treatment. Synthesized condition; 9.5 GPa and 1750 °C for 20 min and (b) sectioned view of as-recovered sample. Synthesized condition: 9.5 GPa and 1600 °C for 20 min.

ing the c-diamond formation was also not changed from the starting condition, as shown in Fig. 8. A summary of quenching experiments is shown in Fig. 9 with a

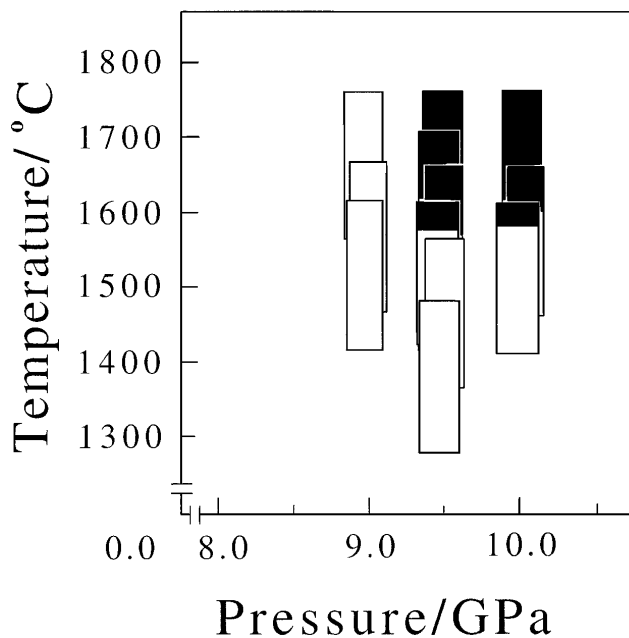


FIG. 6. c-diamond synthesis region for the system graphite-MgCO<sub>3</sub>. (■) c-diamond and (□) graphite.

similar procedure as in Fig. 6. Formation of c-diamond can be seen above 1650 °C and the 9.0–10 GPa region in the system graphite-K<sub>2</sub>Mg(CO<sub>3</sub>)<sub>2</sub>. In the system K<sub>2</sub>CO<sub>3</sub>–MgCO<sub>3</sub>, a peritectic relationship is expected according to the previous investigation.<sup>8,20,21</sup> The estimated melting temperature in the system K<sub>2</sub>Mg(CO<sub>3</sub>)<sub>2</sub> is about 1500 °C at 9 GPa, as expected from extrapolation around the 3–5 GPa region.<sup>20,21</sup> It can be seen, therefore, that c-diamond formation in the system has taken place in the liquid phase of the catalytic component.

SEM photographs for a sample from the system graphite-K<sub>2</sub>Mg(CO<sub>3</sub>)<sub>2</sub> are shown in Figs. 10(a)–10(c). The photographs were also taken near the central axis region at the hot end of the sample. It can be seen that the synthesized c-diamond was covered and/or mixed with fine-grained carbonate of the quenched product, as shown in Fig. 10(a). As the viscosity of the melt K<sub>2</sub>Mg(CO<sub>3</sub>)<sub>2</sub> is extremely low,<sup>22</sup> the melt phase could easily infiltrate the grain boundaries of graphite and/or synthesized c-diamond. Synthesized c-diamond grains can be clearly seen only after the acid treatment, as shown in Fig. 10(b). The synthesized c-diamond grain with this system exhibited an average size of 2–5 μm with an octahedral and/or cubo-octahedral morphology, as shown in Fig. 10(c).

#### D. δ<sup>13</sup>C isotope analysis for the synthesized c-diamond

Table I summarizes the δ<sup>13</sup>C isotope ratios of graphite powder, graphite capsule, and carbonates as the starting material and that of the synthesized c-diamond.

Calculated δ<sup>13</sup>C values in c-diamond are also shown under the assumption that all the molecular carbon in the carbonate transforms to the c-diamond in the present system. The difference between the measured and the calculated value of δ<sup>13</sup>C in c-diamond suggests that the carbon source to form the c-diamond in both carbonate catalyst systems originated from the graphite starting materials. In both systems, therefore, no exchange seems to have occurred between the molecular carbon in the carbonate and elemental carbon. However, if only a small amount of carbon in the carbonate was related to the formation of c-diamond, such a contribution should not sufficiently appear in the measured value of δ<sup>13</sup>C in the c-diamond.

#### IV. DISCUSSION

It can be seen with both graphite-carbonate systems, lower temperature boundaries of the formation of c-diamond were reduced to 1600–1650 °C at the 9–10 GPa region, while the formation of c-diamond with reported carbonate systems required 2000 °C at the 7.7 GPa region. The microstructures of the recovered products and expected melting temperature of each carbonate imply that the state of MgCO<sub>3</sub> as catalytic component was solid, while that of K<sub>2</sub>Mg(CO<sub>3</sub>)<sub>2</sub> was liquid during the period of formation of c-diamond at the 9–10 GPa region. This suggests that the formation mechanism of c-diamond in both of the graphite-carbonate systems is different from each other in the 9–10 GPa region.

In the system graphite-K<sub>2</sub>Mg(CO<sub>3</sub>)<sub>2</sub>, graphite may have dissolved into liquid K<sub>2</sub>Mg(CO<sub>3</sub>)<sub>2</sub> and could precipitate as diamond crystal. In this case, therefore, K<sub>2</sub>Mg(CO<sub>3</sub>)<sub>2</sub> acted as catalytic solvent similar to conventional metal catalysts. This process seems to be similar to that of reported studies of other graphite-inorganic compound systems.<sup>1–6</sup> While each carbonate component in the system of K<sub>2</sub>CO<sub>3</sub> and MgCO<sub>3</sub> exhibited the catalytic effect to form c-diamond above 2000 °C at the 7.7 GPa region,<sup>1</sup> the binary carbonate system of K<sub>2</sub>Mg(CO<sub>3</sub>)<sub>2</sub> synthesizes c-diamond above 1650 °C at the 9 GPa region. Such a reduction of temperature to form c-diamond may be attributed to the reduction of melting temperature due to the peritectic relationship with this binary carbonate system. Further work is, however, required to clarify the pressure-dependence of the c-diamond formation process in molten K<sub>2</sub>Mg(CO<sub>3</sub>)<sub>2</sub>.

In the system graphite-MgCO<sub>3</sub>, the catalytic component of MgCO<sub>3</sub> seems to be in a solid state. The formation mechanism of c-diamond in this system is not clarified at present. An important result is, however, the observation of a pressure threshold for c-diamond formation in this system at about 9.5 GPa, as shown

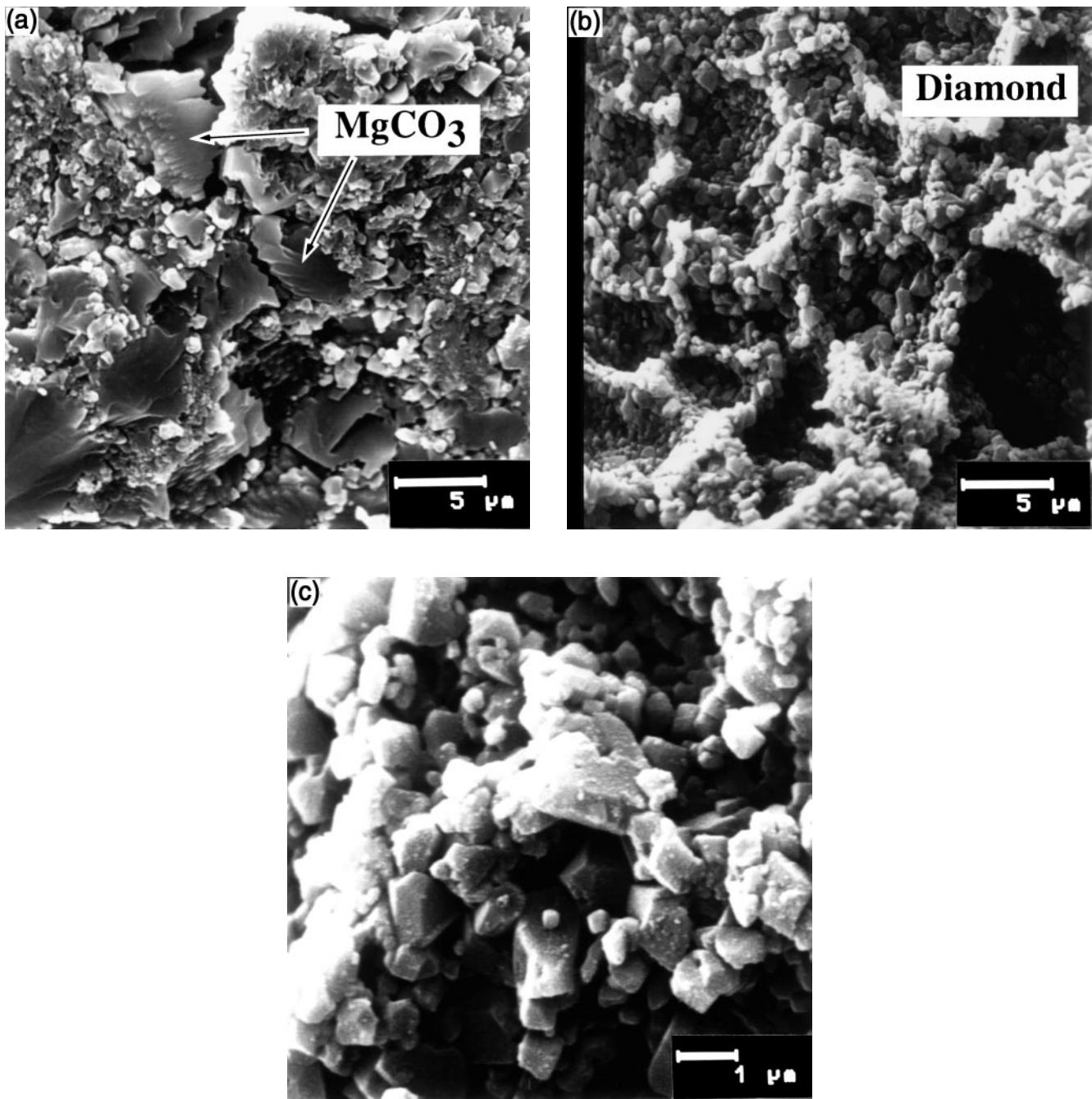


FIG. 7. SEM photographs of the quenched products of the system graphite-MgCO<sub>3</sub> treated at 9.5 GPa and 1650 °C for 20 min. (a) As-recovered without acid treatment, and (b) and (c) after acid treatment to dissolve the carbonate.

in Fig. 6. Furthermore, the evaluated P-T condition required to form c-diamond in this system was located at higher pressure and lower temperature as compared to that in the system graphite-K<sub>2</sub>Mg(CO<sub>3</sub>)<sub>2</sub>. The shear stress in the graphite with the liquid state component of K<sub>2</sub>Mg(CO<sub>3</sub>)<sub>2</sub> should be smaller than that with the solid state component of MgCO<sub>3</sub>. These facts imply that c-diamond formation in the system graphite-MgCO<sub>3</sub> is

sensitive to the compressed state of the graphite, which was affected by the amplitude of pressure and shear stress. By comparison with the state of graphite powder at 9.5 GPa to that at 7.7 GPa, the former seems to be partially transformed to h-diamond, as mentioned previously.

On the other hand, no diamond has been observed from the recovered product with the system graphite-

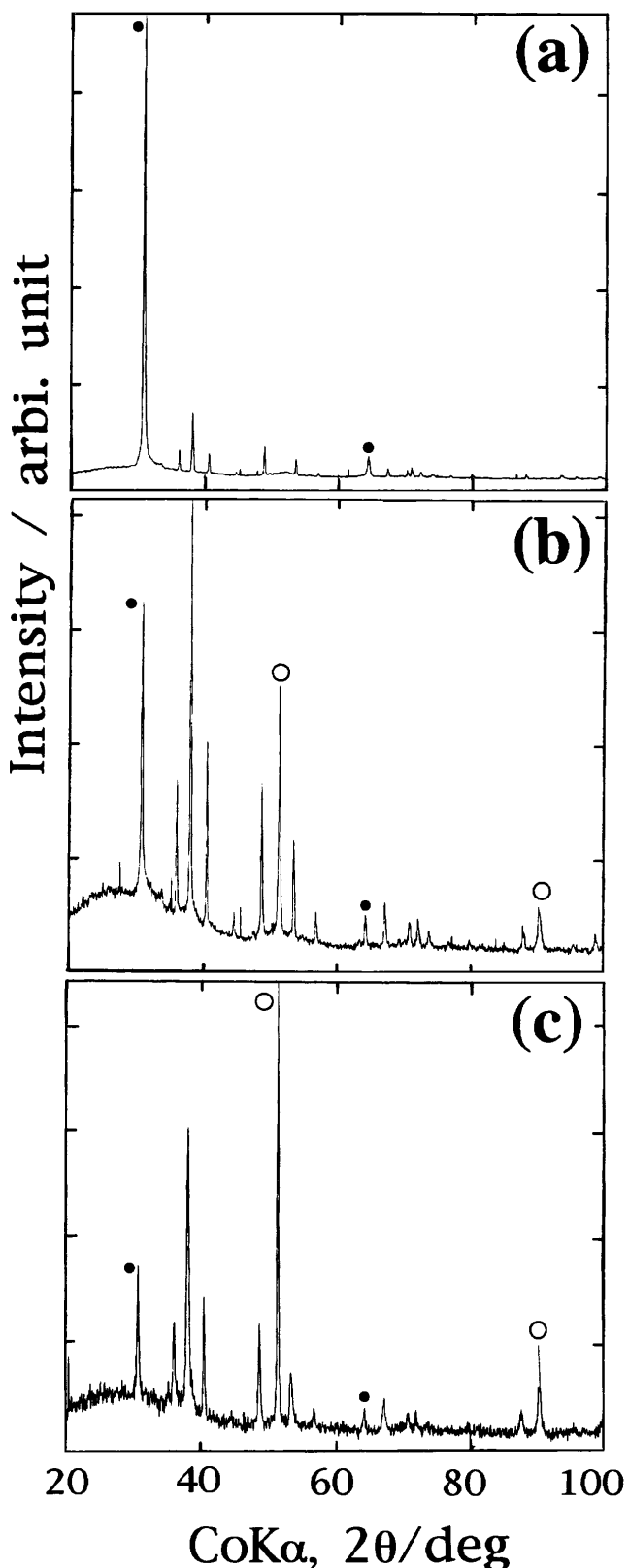


FIG. 8. X-ray diffraction profiles of the system graphite- $\text{K}_2\text{Mg}(\text{CO}_3)_2$ . (a) HP/HT treatment at 9 GPa and 1600 °C for 20 min, (b) 9 GPa and 1650 °C for 20 min, and (c) 9 GPa and 1750 °C for 20 min. (●) graphite and (○) c-diamond.

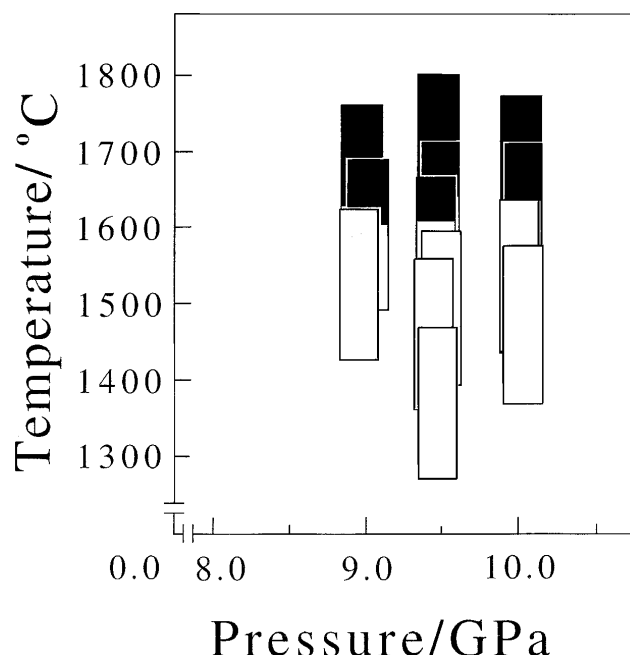


FIG. 9. c-diamond synthesis region for the system graphite- $\text{K}_2\text{Mg}(\text{CO}_3)_2$ . (■) c-diamond and (□) graphite.

calcium carbonate ( $\text{CaCO}_3$ ) and graphite-magnesium oxide ( $\text{MgO}$ ) at similar conditions (9.5 GPa and 1650 °C). Since both the components of  $\text{CaCO}_3$  and  $\text{MgO}$  should also be in solid state at this condition, the presence of  $\text{MgCO}_3$  may, therefore, enhance the formation of c-diamond. In order to consider further possible mechanism of c-diamond formation in this system, the effect of a volatile component in the reaction system might be taken into account, as in the system graphite-water in which growth of diamond took place.<sup>5</sup> Comparing  $\text{MgCO}_3$  with  $\text{MgO}$  and  $\text{CaCO}_3$ , the decomposition temperature at ambient atmosphere of the former is seen to be lower than that of the latter.<sup>23</sup> At high pressure, however, previous research did not show the evidence of free- $\text{CO}_2$  in liquid  $\text{MgCO}_3$  above 8 GPa.<sup>19</sup> According to the x-ray diffraction profiles, there is no discernible evidence of the formation of  $\text{MgO}$  in the recovered products in the system graphite- $\text{MgCO}_3$  in this study. Further investigation such as *in situ* observation using x-ray diffraction<sup>24</sup> might reveal the process of c-diamond formation, including a more precise assessment of any volatile component in the system under HP/HT.

The lower limit of the temperature to produce c-diamond in the system graphite- $\text{MgCO}_3$  was 1600 °C at 10 GPa region, which may be close to a geotherm of an off-craton area, but is still higher than that of a craton area.<sup>25</sup> To attain the aim of lowering the synthesis temperature and pressure of the c-diamond with the system graphite-carbonate, establishments of the system

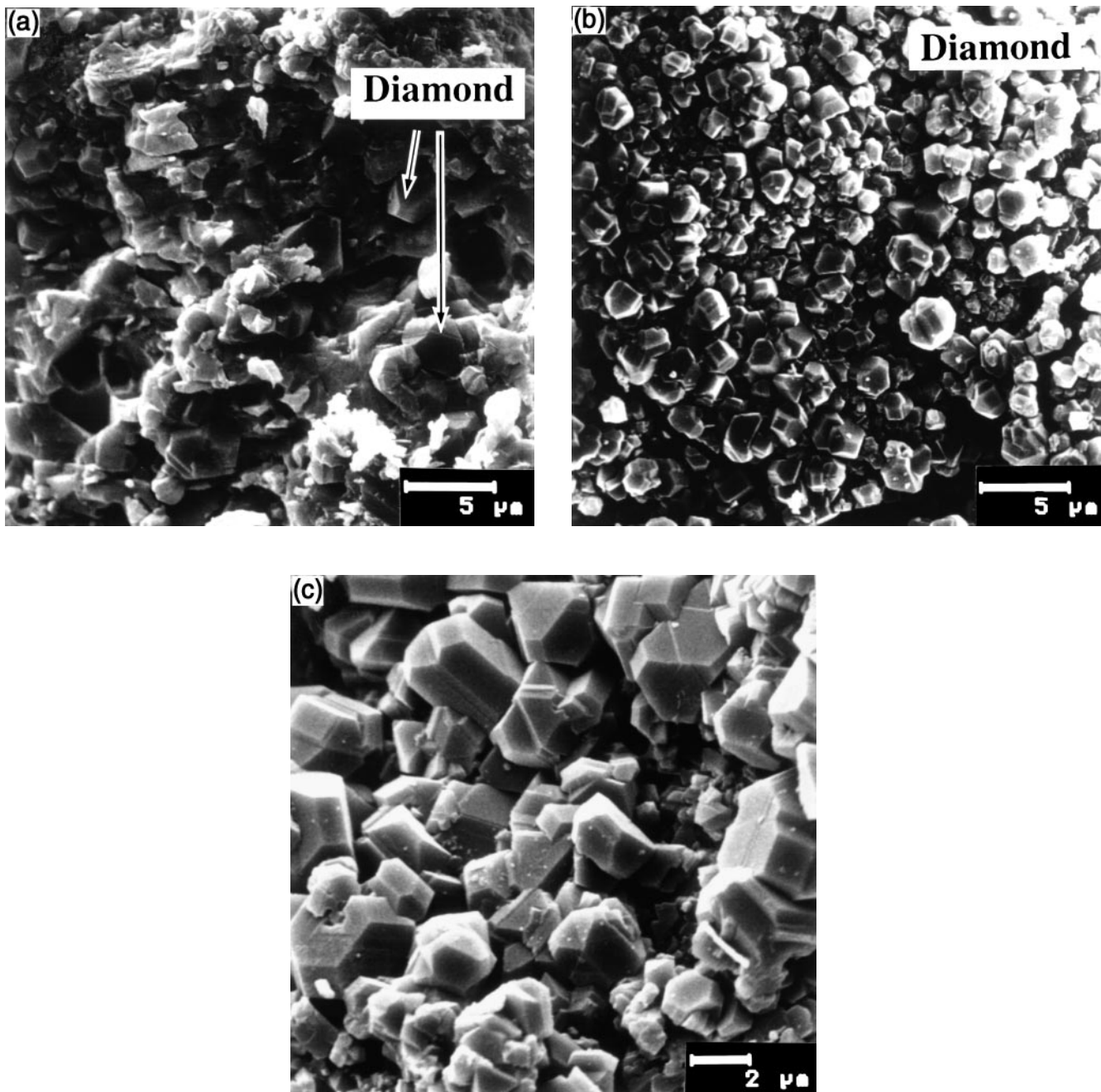


FIG. 10. SEM photographs of the quenched products of the system graphite- $K_2Mg(CO_3)_2$  treated at 9.0 GPa and 1650 °C for 20 min. (a) As-recovered without acid treatment, and (b) and (c) after acid treatment to dissolve the carbonate. Grain of c-diamond is indicated by arrows in (a).

for a well-controlled volatile component seems to be the most important factor for the future work.

## V. CONCLUSIONS

(1) Above 9.5 GPa and 1600 °C, natural magnesite ( $MgCO_3$  from NSW) exhibits a catalytic effect for conversion of c-diamond from graphite and/or h-diamond.

There is a major pressure threshold in the system at 9.5 GPa above which diamond nucleation temperatures are reduced to 1600 °C.

(2) Above 9 GPa and 1650 °C,  $K_2Mg(CO_3)_2$  (melt) exhibits a catalytic effect for conversion of c-diamond from graphite and/or h-diamond.

(3) Recovered graphite from 9–9.5 GPa and 1750 °C region exhibits a trace of compressed graphite and broad peaks of h-diamond.

TABLE I. Summary of carbon isotope  $\delta^{13}\text{C}$  values.

Specimen	$\delta^{13}\text{C}$ (measured)	$\delta^{13}\text{C}$ (calculated) <sup>b</sup>
Graphite powder	-23.65	
Graphite rod	-24.59	
$\text{K}_2\text{Mg}(\text{CO}_3)_2$	-15.63	
$\text{MgCO}_3$ (NSW)	-7.13	
$\text{MgCO}_3$ (California)	-1.71	
$\text{MgCO}_3$ (Lab made)	-14.84	
Diamond I <sup>a</sup>	-24.43	-22.8
Diamond II <sup>a</sup>	-23.40	-22.1
Diamond III <sup>a</sup>	-23.82	-21.3
Diamond IV <sup>a</sup>	-23.36	-23.2

<sup>a</sup>Analysis has been made for purified c-diamond. Carbonate and remained graphite in the recovered product were dissolved by a hot aqua regia and a hot mixture of  $\text{HNO}_3$  and  $\text{H}_2\text{SO}_4$ , respectively. All the diamond specimens were synthesized at 9.5 GPa and 1700 °C for 20 min in the following system: I: graphite- $\text{K}_2\text{Mg}(\text{CO}_3)_2$  system, II: graphite- $\text{MgCO}_3$  (NSW) system, III: graphite- $\text{MgCO}_3$  (California) system, and IV: graphite- $\text{MgCO}_3$  (Lab made<sup>10</sup>) system.

<sup>b</sup>Under the assumption that all the carbon of the carbonate in this system transform to diamond.

(4) It can be seen from the carbon isotope analyses for  $\delta^{13}\text{C}$  in both the systems graphite- $\text{MgCO}_3$  and graphite- $\text{K}_2\text{Mg}(\text{CO}_3)_2$  that the carbon source for the synthesized diamond originated from the graphite starting powder and not the carbonates.

(5) If natural diamond forms in the presence of magnesite, or other carbonates (including melt) in the Earth's mantle, then our data suggest that pressures above 9 GPa may be more favorable since our synthesis conditions are rather close to a normal geotherm.

## ACKNOWLEDGMENTS

The authors would like to acknowledge Dr. I. G. Wood of University College London (UCL) for his help in x-ray diffraction study; Mr. P. A. Woods, Mr. S. Houlding, and Mr. J. Huggett of UCL for their help in the experimental study; Mr. J. Sowerby of UCL for his help in the IR spectroscopy analysis; Mr. J. Davy and Mr. T. Stiles of UCL for their SEM analysis; and Dr. W. R. Taylor of UCL for his help in IR analysis and useful discussions in this study. We also thank Professor C. T. Pillinger of Open University for performing the carbon isotope analysis. We acknowledge Mr. S. Takenouchi of National Institute for Research in Inorganic Materials (NIRIM) for the ICP analysis. We thank Dr. M. Akaishi of NIRIM for supplying the laboratory-made  $\text{MgCO}_3$  powder. We also thank Dr. S. Varanasi, Dr. H. Yamada, Dr. H. Kanda, Dr. M. Akaishi, and Dr. S. Yamaoka of NIRIM for their useful comments for improving this manuscript. The British Council is thanked for travel support at an

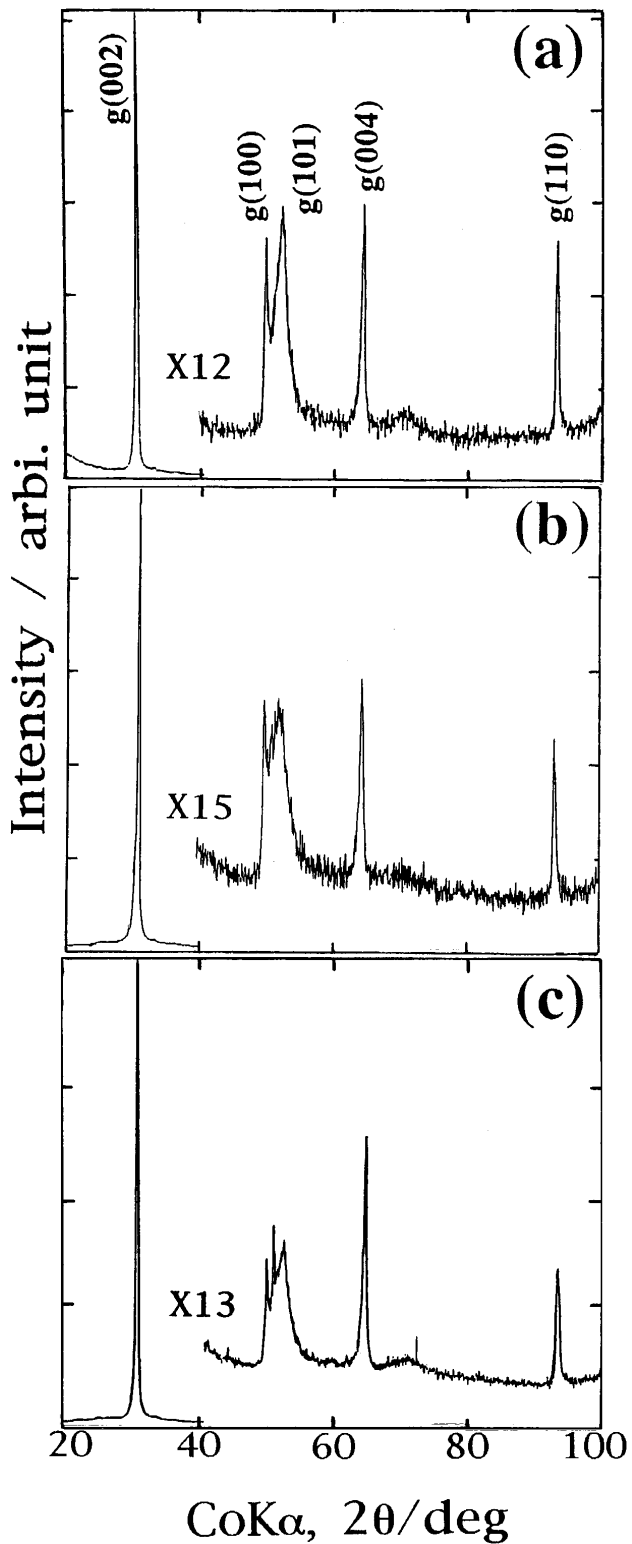


FIG. 11. X-ray diffraction profiles of the powdered graphite rod. (a) Starting condition, (b) HP/HT treatment at 9.5 GPa and 1550 °C for 20 min, and (c) 9.5 GPa and 1750 °C for 20 min.

important stage in the development of this joint London-Tsukuba collaborative program.

## REFERENCES

1. M. Akaishi, H. Kanda, and S. Yamaoka, *J. Cryst. Growth* **104**, 578 (1990).
2. M. Akaishi, H. Kanda, and S. Yamaoka, *Jpn. J. Appl. Phys.* **29**, L1172 (1990).
3. M. Akaishi, *Diamond and Related Materials* **2**, 183 (1993).
4. H. Kanda, M. Akaishi, and S. Yamaoka, *J. Cryst. Growth* **106**, 471 (1990).
5. S. Yamaoka, M. Akaishi, and H. Kanda, *J. Cryst. Growth* **125**, 375–377 (1992).
6. M. Arima, K. Nakayama, M. Akaishi, S. Yamaoka, and H. Kanda, *Geology* **21**, 968 (1993).
7. H. P. Bovenkerk, F. P. Bundy, H. T. Hall, H. M. Strong, and R. H. Wentorf, Jr., *Nature* **184**, 1094 (1959).
8. S. E. Ragone, *J. Phys. Chem.* **70**, 3361 (1966).
9. J. Thomas, Jr., N. E. Weston, and T. E. O'Conner, *J. Am. Chem. Soc.* **84**, 4619 (1963).
10. Similar quality used in previous study<sup>1,3</sup> (supplied by Dr. M. Akaishi).
11. S. J. Matthews, A. P. Jones, and A. D. Beard, *J. Geological Soc. London* **151**, 815 (1994).
12. B. Simons, *J. Appl. Cryst.* **16**, 143 (1983).
13. D. Walker, C. A. Carpenter, and C. M. Hitch, *Am. Mineralogist* **75**, 1020 (1990).
14. A. Onodera, *High Temp.–High Press.* **19**, 579 (1987).
15. T. Yagi, M. Akaogi, O. Shimomura, T. Suzuki, and S. Akimoto, *J. Geophys. Res.* **92 B7**, 6207 (1987).
16. T. Yagi and S. Akimoto, *Technophysics* **35**, 259 (1976).
17. G. P. Bery and T. Kohler, *J. Petrology* **31**, 1353 (1990).
18. M. M. Grady, I. P. Wright, P. K. Swart, and C. T. Pillinger, *Geo. Cosmo. Acta* **52**, 2885 (1988).
19. T. Katsura and E. Ito, *Earth and Planetary Sci. Lett.* **99**, 110 (1990).
20. A. P. Jones and M. G. Genge, *Proc. of AGU 1994 Fall Meeting* **75**, 725 (1994).
21. D. Dobson and A. P. Jones, unpublished work.
22. A. P. Jones, D. Dobson, R. Rabe, M. Kanzaki, T. Kondo, K. Kurita, T. Sekine, O. Shimomura, T. Taniguchi, and S. Urakawa, *PF Activity Rept.* 92-G289 437 (1993).
23. G. J. Janz, *Molten Salts Handbook* (Academic Press, New York, 1967), p. 20.
24. T. Kikegawa, O. Shimomura, H. Iwasaki, S. Sato, A. Mikuni, A. Iida, and N. Kamiya, *Rev. Sci. Instrum.* **60**, 1527 (1989).
25. D. S. Chapman and H. N. Pollack, *Geology* **5**, 265 (1977).
26. F. P. Bundy and J. S. Kasper, *J. Chem. Phys.* **46**, 3437 (1967).
27. T. Yagi, W. Utsumi, A. Yamakata, T. Kikegawa, and O. Shimomura, *Phys. Rev. B* **46**, 6031 (1992).

## VIII. APPENDIX

Figure 11 shows the x-ray diffraction profiles of a powdered graphite rod used for the capsule initially and after HP/HT treatment. The graphite machined from the rod has not undergone the transformation to a denser phase at this HP/HT condition. It was, therefore, possible to use graphite as the furnace to produce stable heating conditions. This implies that the graphite with poorer initial crystallinity as shown by an infinite G.I. value was not easily transformed to a denser phase, as noted by many researchers.<sup>26,27</sup>